Electronic Supplementary Material (ESI) for Environmental Science: Nano.
This journal is © The Royal Society of Chemistry 2021

Electronic Supplementary Information

Enhanced degradation of norfloxacin by Ce-mediated Fe-MIL-101: Catalytic mechanism, degradation pathways, and potential applications in wastewater treatment

Chaosheng Bao,‡[a] Jian Zhao,‡[bc] Yuanyuan Sun,[a] Xiaoliang Zhao,[a] Xiaohui Zhang,[a] Yukun Zhu,[a] Xilin She,[a] Dongjiang Yang,*[,ad] and Baoshan Xing[e]

[a] *School of Environmental Science and Engineering, School of Materials Science and Engineering, State Key Laboratory of Bio-fibers and Eco-textiles, Shandong Collaborative Innovation Center of Marine Biobased Fibers and Ecological Textiles, Institute of Marine Biobased Materials, Qingdao University, Qingdao 266071, China. E-mail: d.yang@qdu.edu.cn (D.J. Yang)*

[b] *Laboratory for Marine Ecology and Environmental Science, Qingdao National Laboratory for Marine Science and Technology, Qingdao 266071, China*

[c] *Institute of Coastal Environmental Pollution Control, Ministry of Education Key Laboratory of Marine Environment and Ecology, Frontiers Science Center for Deep Ocean Multispheres and Earth System, Ocean University of China, Qingdao 266100, China*

[d] *Queensland Micro- and Nanotechnology Centre (QMNC), Griffith University, Nathan Campus, Brisbane, Queensland 4111, Australia*

[e] *Stockbridge School of Agriculture, University of Massachusetts, Amherst, Massachusetts 01003, United States*

* Corresponding authors

‡ C. B. and J. Z. contributed equally to this work.

Table of Contents

S1. Supplemental Materials and Methods

Text S1. Materials and reagents.

Text S2. Analytical Methods.

Text S3. Identification of degradation intermediates and pathways.

Text S4. The kinetic analyses of the degradation data.

S2. Supplemental results and discussion

Table S1. Metal content ratio of Fe to Ce in different Fe/Ce-MIL-101 catalysts.

Table S2. Specific Surface Area and Pore Characteristics of Fe-MIL-101 and Fe/Ce-MIL-101.

Table S3. Adsorption capacity of Fe/Ce-MIL-101 for NOR.

Table S4. Comparison of the Fenton-Like catalytic activity between Fe/Ce-MIL-101-5% and various efficient Catalysts reported in literature.

Table S5. The bond length of Fe-O and Ce-O, and the bond angel of Fe-O-Fe and Fe-O-Ce are listed.

Table S6. The calculation results of H_2O_2 adsorption on Fe_3 and Fe_2Ce clusters. The adsorption energy Eads and charge transfer Q between H_2O_2 and cluster are listed.

Table S7. The intermediates of NOR degradation after 20-min and 180-min degradation.

Fig. S1 (a) FESEM image, (b) and (c) TEM image of Fe-MIL-101.

Fig. S2 The XPS spectra of (a) survey scans and (b) Ce 3d of Fe-MIL-101 and Fe/Ce-MIL-101-5%.

Fig. S3 (a) N_2 adsorption−desorption isotherms and (b) relative pore size-distribution profiles spectra of Fe-MIL-101 and Fe/Ce-MIL-101-5%.

Fig. S4 (a) The removal rate of Fe/Ce-MIL-101 only for NOR. (b) The adsorption isotherms of NOR uptake by Fe/Ce-MIL-101. Experiments reaction conditions: [NOR]=10 mg/L, [H_2O_2]=20 mM, catalyst=0.3 g/L, T=25 °C, initial solution pH=7.0.

Fig. S5 The reaction rate constant for NOR degradation over Fe-MIL-101 and Fe/Ce-MIL-101.

Fig. S6 (a) Iron leakage with different pH in Fe/Ce-MIL-101-5%-H_2O_2 system. (b) Removal efficiency of NOR by homogeneous Fenton and heterogeneous Fenton at pH 3.

Fig. S7 (a) High magnification and (b) low magnification FESEM images of Fe/Ce-MIL-101 after reaction.

Fig. S8 XRD spectra of Fe/Ce-MIL-101 before and after reaction.

Fig. S9 XPS spectra of Fe/Ce-MIL-101-5% and Fe-MIL-101: (a) survey scan, (b) C 1s.

S1. Supplemental Materials and Methods

Text S1. Materials and reagents.

N,N-Dimethylformamide (DMF) was bought from Tianjin Beilian Fine Chemical (Tianjin, China). $Ce(NO_3)_3 \cdot 6H_2O$ was purchased from Adamas Reagent (Shanghai, China). 1,4-dicarboxybenzene (H_2BDC), sulfamethazine (SMT), bisphenol A (BPA), and Norfloxacin (NOR) was supplied by Aladdin Chemistry (Shanghai, China). Iron chloride hexahydrate ($FeCl_3 \cdot 6H_2O$), hydrogen peroxide (H_2O_2, 30wt%), ethanol (C_2H_5OH), tert-butyl alcohol (TBA), p-benzoquinone (BQ), hydrochloric acid (HCl), sodium hydroxide (NaOH), and phosphoric acid (H_3PO_4) were purchased from Sinopharm Chemical Reagent Co., Ltd., (Beijing, China). Methanol was bought from Sinopharm Chemical Reagent high-performance liquid chromatography (HPLC) grade, while acetonitrile was purchased from Cinc HPLC grade. Other drugs were analytically pure.

Text S2. Analytical Methods.

The concentration of NOR, BPA, and SMT in the extracted solution was analyzed using L6 high-performance liquid chromatography (HPLC, Persee, China) with a UV detector and an Agela C18 column (5 μm, 4.6 × 150 mm). The detection wavelengths of NOR, BPA, and, SMT were set to 278, 224, and 275 nm, respectively. The mobile phase consisted of 0.2% phosphoric acid/acetonitrile (80:20), methanol/water (75:25), and acetonitrile/water (65:35) for NOR, BPA, and SMT, respectively, and the flow rate was set to 0.7 mL/min. The dissolved concentrations of iron ion at different pH were detected by Avio 200 Inductive Coupled Plasma Optical Emission Spectrometer (ICP-OES, PerkinElmer, USA). The solution to be tested was taken from the Fe/Ce-MIL-101/H_2O_2 system and filtered with a 0.22 μm membrane.

Text S3. Identification of degradation intermediates and pathways.

Density functional theory (DFT) calculations of degradation pathways were performed by Gaussian 09 program.[1] And atoms energy calculations were performed at B3LYP-D3BJ/def2-SV(P) level[2]. The solvation model of density (SMD) implicit solvation model[3] was used to take account of the solvation effect of water. The condensed electrostatic potential (ESP) mapped molecular surface was obtained by the Multiwfn program[4]. The Fukui function was introduced to describe the nucleophilic, electrophilic, and radical attacks.[5] The simplified Fukui function corresponding to the above three situations are as follows:

Nucleophilic: $f_k^+ = q_N^k - q_{N+1}^k$

Electrophilic: $f_k^- = q_{N+1}^k - q_N^k$

Radical: $f_k^0 = (q_{N-1}^k - q_{N+1}^k)/2$

Where k is the number of atoms used in the calculation, N is the number of electrons in the current state, and q^k represents the atomic charge population number of the atom k. In this study, free radical reaction is the most important mechanism, so f^0_k of NOR molecule was employed to study the degradation pathway. The greater the value of f^0_k, the more vulnerable the site is to free radical attack.

Text S4. The kinetic analyses of the degradation data.

The pseudo-first-order kinetic model was used to fit the curves of NOR degradation by Fe-MIL-101 and Fe/Ce-MIL-101. The degradation curves can fit with the equations:

$-\ln (C_t/C_0)=kt$

where,

C_0: NOR concentration at the time of t=0 (mg/L);

C_t: NOR concentration at the time of t=t (mg/L);

t: degradation reaction time (min);

k: degradation reaction rate constant (min^{-1}).

S2. Supplemental results and discussion

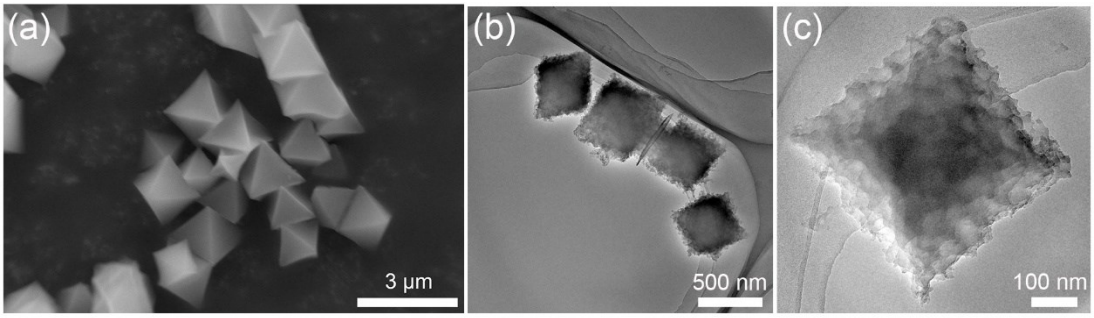

Fig S1. (a) FESEM image, (b) and (c) TEM image of Fe-MIL-101.

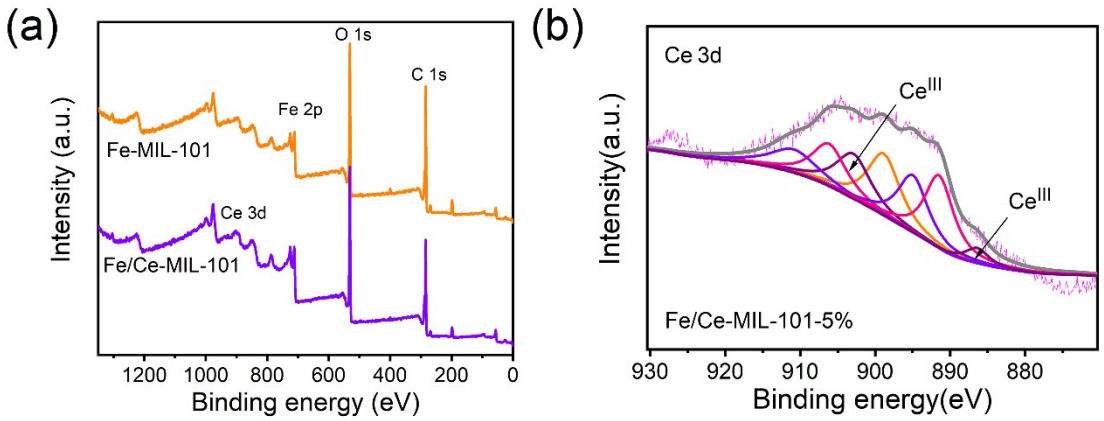

Fig S2. The XPS spectra of (a) survey scans and (b) Ce 3d of Fe-MIL-101 and Fe/Ce-MIL-101-5%.

Table S1. Metal content ratio of Fe to Ce in different Fe/Ce-MIL-101 catalysts.

Catalysts	Fe		Ce	
	Concentration (mg/L)	Proportion	Concentration (mg/L)	Proportion
Fe/Ce-MIL-101-3%	55.28	95.7%	2.47	4.3%
Fe/Ce-MIL-101-5%	22.34	93.4%	1.58	6.6%
Fe/Ce-MIL-101-7%	42.18	91.7%	3.82	8.3%
Fe/Ce-MIL-101-10%	46.42	87.0%	6.91	13.0%

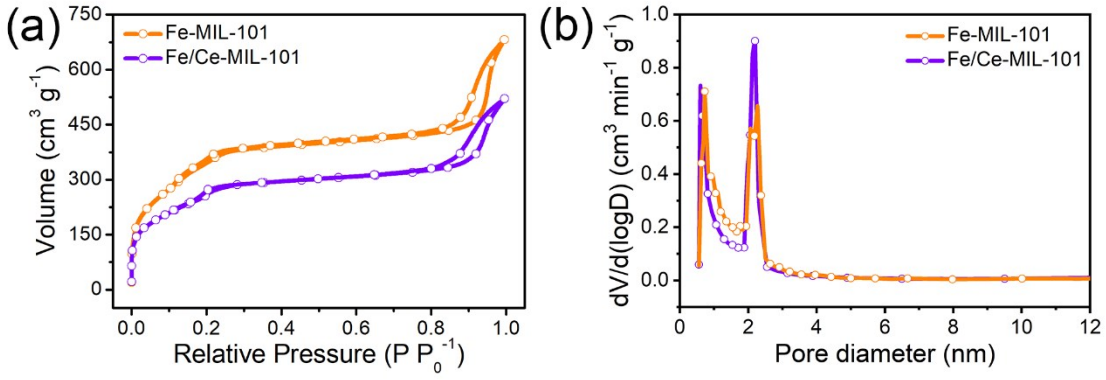

Fig S3. (a) N_2 adsorption-desorption isotherms and (b) relative pore size-distribution profiles spectra of Fe-MIL-101 and Fe/Ce-MIL-101-5%.

Table S2. Specific Surface Area and Pore Characteristics of Fe-MIL-101 and Fe/Ce-MIL-101.

Sample	S_{BET} (m^2/g)	Average pore diameter (nm)	Total pore volume (cm^3/g)
Fe-MIL-101	**1268.01**	**3.325**	**1.054**
Fe/Ce-MIL-101	**922.25**	**3.491**	**0.805**

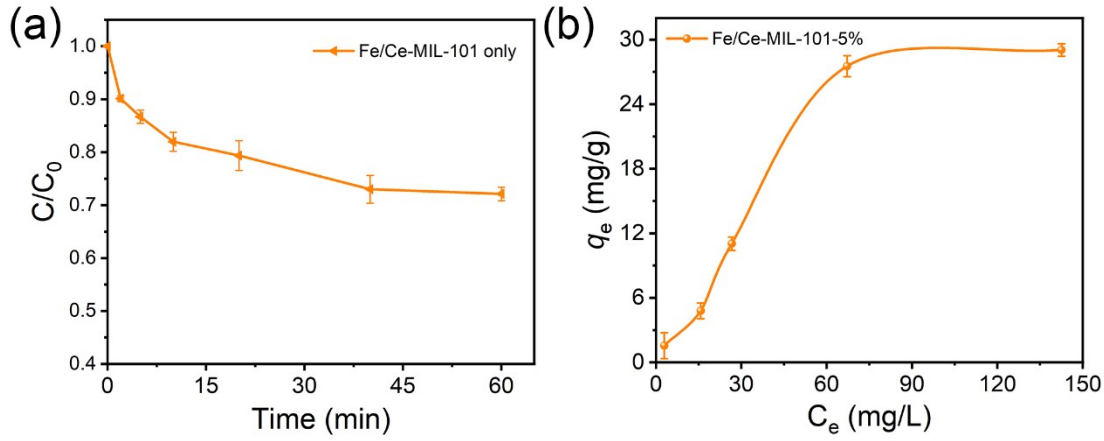

Fig S4. (a) The removal rate of Fe/Ce-MIL-101 only for NOR. (b) The adsorption isotherms of NOR uptake by Fe/Ce-MIL-101. Reaction conditions: [NOR]=10 mg/L, catalyst=0.3 g/L, T=25 °C, initial solution pH=7.0.

Table S3. Adsorption capacity of Fe/Ce-MIL-101 for NOR.

Sample	Langmuir constants			Freundlich constants		
	q_m (mg/g)	K_l (L/mg)	R^2	K_F (mg/g(L/mg)$^{1/n}$)	n	R^2
Fe/Ce-MIL-101	**47.393**	**0.013**	**0.906**	**1.623**	**0.823**	**0.970**

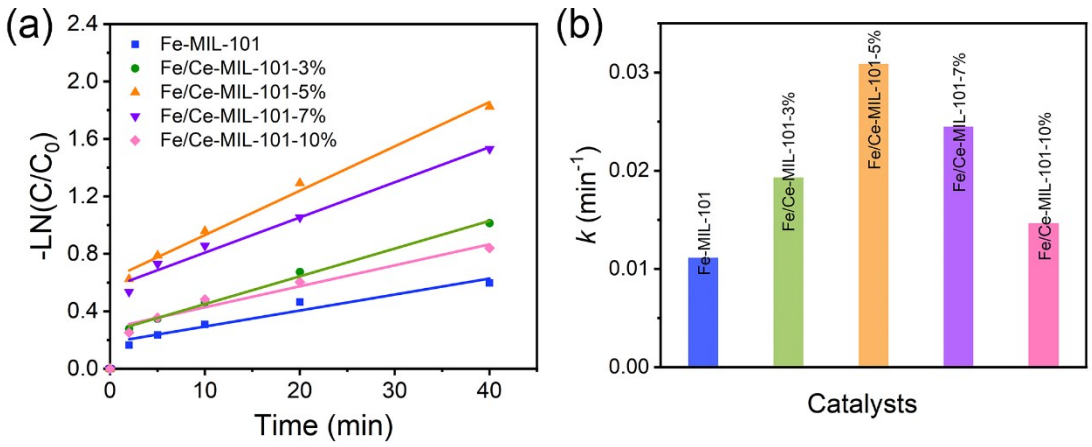

Fig S5. (a) The reaction rate constant and (b) *k* values for NOR degradation over Fe-MIL-101 and Fe/Ce-MIL-101.

Table S4. Comparison of the Fenton-Like catalytic activity between Fe/Ce-MIL-101-5% and various efficient catalysts reported in literatures.

Target pollutants	Catalysts	Reaction conditions	Catalytic performance	References
Norfloxacin (NOR)	Fe/Ce-MIL-101-5%	catalyst: 0.3 g L^{-1}, H_2O_2: 20 mM, NOR: 10 mg L^{-1}, T: 25 °C, pH: 7.0.	94.8% removal in 60 min	This work
Norfloxacin (NOR)	$MnFe_2O_4$	catalyst: 0.6 g L^{-1}, H_2O_2: 200 mM, NOR: 10 mg L^{-1}, T: 25 °C, pH: 6.6.	90.6% removal in 180 min	6
Norfloxacin (NOR)	magnetite nanoparticles	catalyst: 0.3 g L^{-1}, PS: 5 mM, NOR: 10 μM, T: 25 °C, pH: 4.0.	80.0% removal in 60 min	7
Norfloxacin (NOR)	$CuFe_2O_4$	catalyst: 0.2 g L^{-1}, PMS: 0.5 mM, NOR: 25 μM, T: 25 °C, pH: 7.0.	90.0% removal in 120 min	8
Norfloxacin (NOR)	BC@nZVI/Ni	catalyst: 0.2 g L^{-1}, PS: 0.4 mM, NOR: 10 mg L^{-1}, T: 30 °C, pH: 3.0.	80.5% removal in 40 min	9
Norfloxacin (NOR)	corn stalk biochar	catalyst: 0.8 g L^{-1}, PS: 3.8 mM, NOR: 10 mg L^{-1}, T: 20 °C, pH: 6.5.	94.2% removal in 300 min	10
Norfloxacin (NOR)	CoPc/GO	catalyst: 0.1 g L^{-1}, PMS: 0.7 mM, NOR: 10 mg L^{-1}, T: 25 °C, pH: 7.0.	80.1% removal in 60 min	11

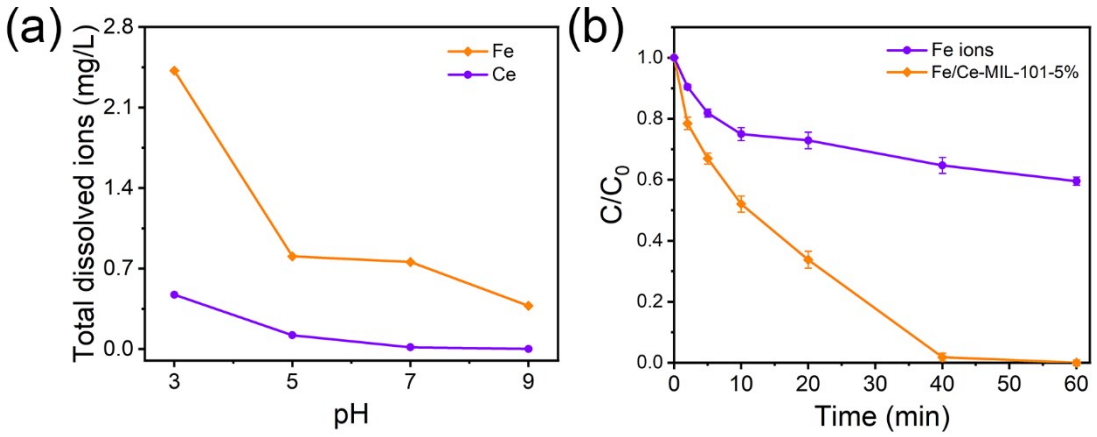

Fig S6. (a) Fe and Ce ion leakage with different pH in Fe/Ce-MIL-101-5%-H_2O_2 system. (b) Removal efficiency of NOR by homogeneous Fenton and heterogeneous Fenton at pH 3.

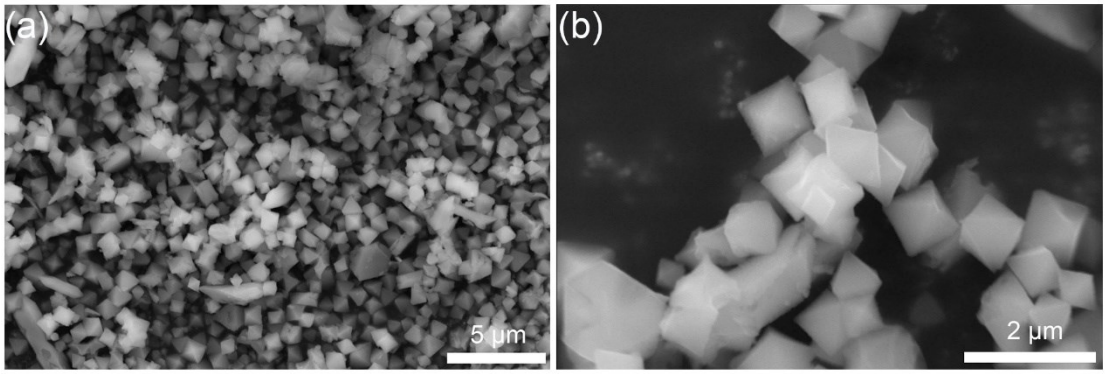

Fig S7. (a) Low magnification and (b) high magnification FESEM images of Fe/Ce-MIL-101 after reaction.

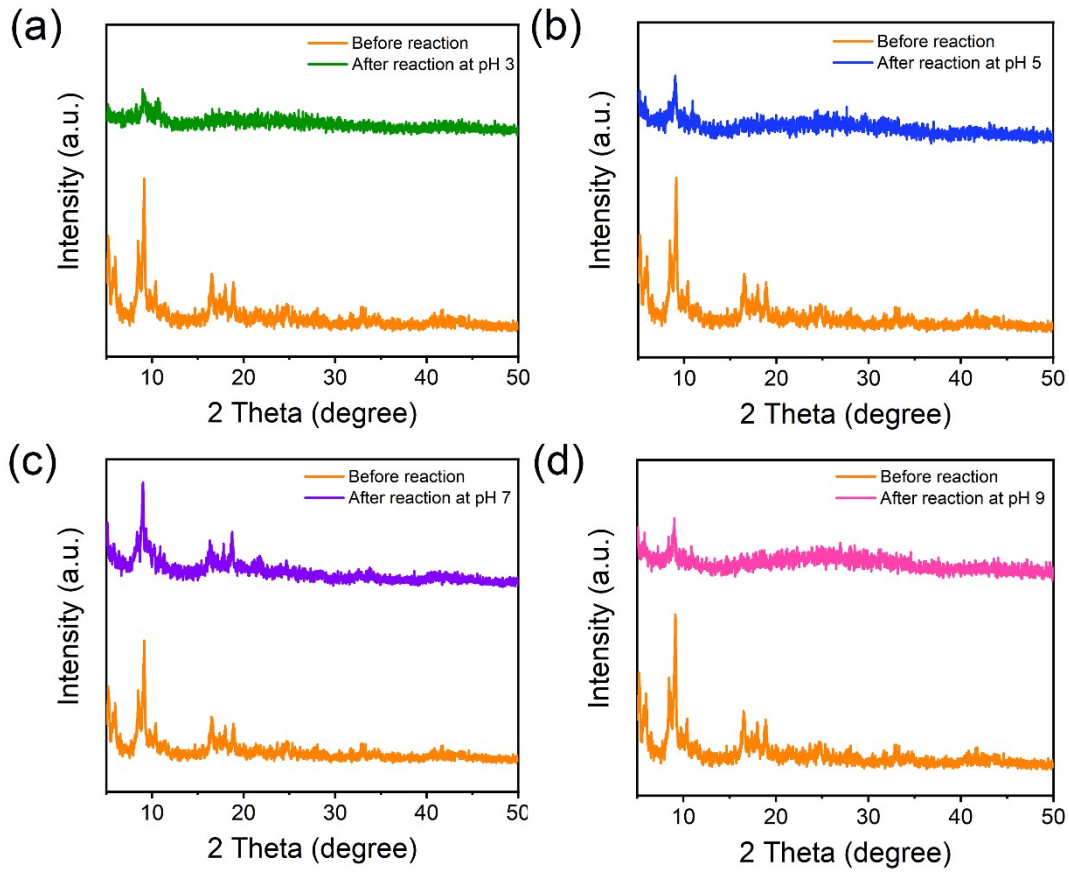

Fig S8. XRD spectra of Fe/Ce-MIL-101 before and after reaction at different pH.

Table S5. The bond length of Fe-O and Ce-O, and the bond angel of Fe-O-Fe and Fe-O-Ce are listed.

Bond type	Bond length (Å)	Bond angel (°)
Fe-O (Fe-O-Fe)	**1.85**	**85.12**
Ce-O (Fe-O-Ce)	**2.15**	**98.43**

Table S6. The calculation results of H_2O_2 adsorption on Fe_3 and Fe_2Ce clusters. The adsorption energy E_{ads} and charge transfer Q between H_2O_2 and cluster are listed.

Structure	E_{ads} (eV)	Q (e)
H_2O_2 - Fe_3 cluster	**0.43**	**-1.37**
H_2O_2 – Fe_2Ce cluster	**0.52**	**-1.48**

Table S7. The intermediates of NOR degradation after 20-min, 60-min and 180-min degradation.

Products	m/z	Ion Formula	Structure	Areas of Intermediates (20 min)	Areas of Intermediates (60 min)	Areas of Intermediates (180 min)	References
NOR	320.1401	$C_{16}H_{19}FN_3O_3$	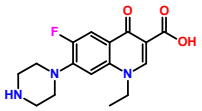				
IM1/IM5	352.1143	$C_{16}H_{18}FN_3O_5$	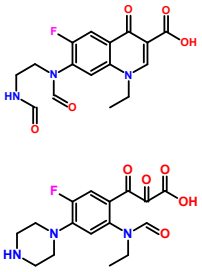	-	-	-	12
IM2	294.1245	$C_{14}H_{17}FO_3N_3$	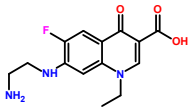	24925.5	19109.8	-	12
IM3	251.0812	$C_{12}H_{11}FN_2O_3$	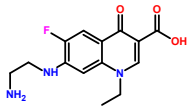	33567.3	35896.6	37116.3	12
IM4	324.1342	$C_{15}H_{19}FN_3O_4$	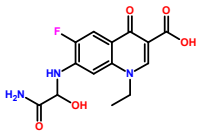	36708.0	23029.5	5512.4	13
IM6	324.1339	$C_{17}H_{17}FN_3O_4$	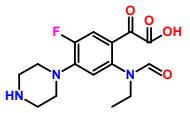	22007.3	2674.8	-	13
IM7	296.1409	$C_{14}H_{18}FN_3O_3$	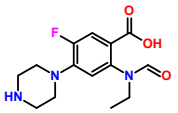	43211.5	72819.3	-	13
IM8	278.1284	$C_{14}H_{16}FN_3O_2$	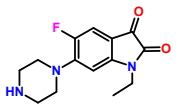	15943.8	17691.6	-	14
IM9	252.1513	$C_{12}H_{14}FN_3O_2$	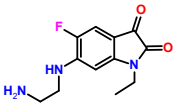	5901.5	10064.1	-	13

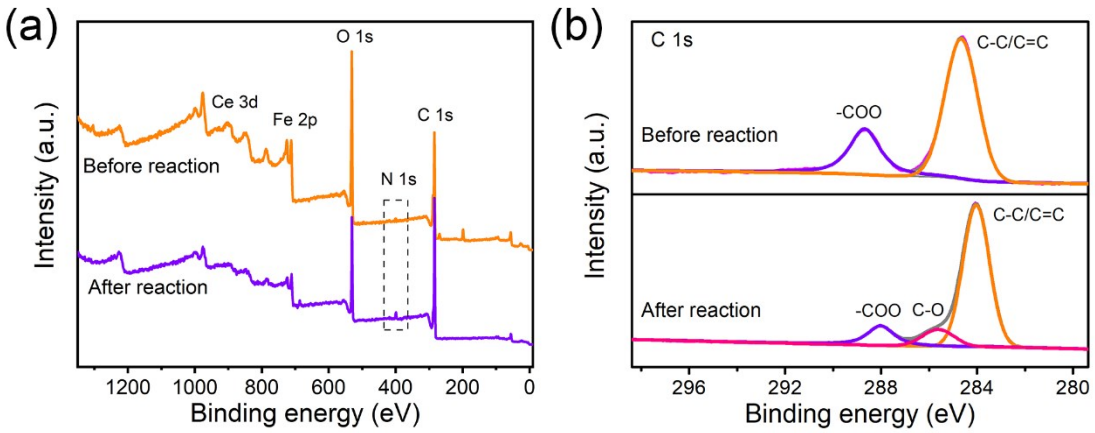

Fig S9. XPS spectra of Fe/Ce-MIL-101-5% before and after reaction: (a) survey scan, (b) C 1s.

References

1. M. J. Frisch, G. W. Trucks, H. B. Schlegel, G. E. Scuseria, M. A. Robb, J. R. Cheeseman, G. Scalmani, V. Barone, G. A. Petersson, H. Nakatsuji, X. Li, M. Caricato, A. Marenich, J. Bloino, B. G. Janesko, R. Gomperts, B. Mennucci, H. P. Hratchian, J. V. Ortiz, A. F. Izmaylov, J. L. Sonnenberg, D. Williams-Young, F. Ding, F. Lipparini, F. Egidi, J. Goings, B. Peng, A. Petrone, T. Henderson, D. Ranasinghe, V. G. Zakrzewski, J. Gao, N. Rega, G. Zheng, W. Liang, M. Hada, M. Ehara, K. Toyota, R. Fukuda, J. Hasegawa, M. Ishida, T. Nakajima, Y. Honda, O. Kitao, H. Nakai, T. Vreven, K. Throssell, J. A. Montgomery, Jr., J. E. Peralta, F. Ogliaro, M. Bearpark, J. J. Heyd, E. Brothers, K. N. Kudin, V. N. Staroverov, T. Keith, R. Kobayashi, J. Normand, K. Raghavachari, A. Rendell, J. C. Burant, S. S. Iyengar, J. Tomasi, M. Cossi, J. M. Millam, M. Klene, C. Adamo, R. Cammi, J. W. Ochterski, R. L. Martin, K. Morokuma, O. Farkas, J. B. Foresman, and D. J. Fox, Gaussian 09, Revision A.02, *Gaussian, Inc.*, Wallingford CT, 2016.
2. S. Grimme, J. Antony, S. Ehrlich and H. Krieg, A consistent and accurate ab initio parametrization of density functional dispersion correction (DFT-D) for the 94 elements H-Pu, *J. Chem. Phys.*, 2010, **132**, 154104.
3. A. V. Marenich, C. J. Cramer and D. G. Truhlar, Universal solvation model based on solute electron density and on a continuum model of the solvent defined by the bulk dielectric constant and atomic surface tensions, *J. Phys. Chem. B.*, 2009**, 113**, 6378.
4. T. Lu and F. Chen, Multiwfn: A multifunctional wavefunction analyzer, *J. Comput. Chem.*, 2012, **33**, 580-592.
5. Y. Wang, H. Sun, H. M. Ang, M. O. Tadé and S. Wang, Magnetic Fe_3O_4/Carbon Sphere/Cobalt Composites for Catalytic Oxidation of Phenol Solutions with Sulfate Radicals, *Chem. Eng. J.*, 2014, **245**, 1-9.
6. G. Wang, D. Zhao, F. Kou, Q. Ouyang, J. Chen and Z. Fang, Removal of norfloxacin by surface Fenton system ($MnFe_2O_4/H_2O_2$): Kinetics, mechanism and degradation pathway, *Chem. Eng. J.*, 2018, **351**, 747-755.

7. D. Ding, C. Liu, Y. Ji, Q. Yang, L. Chen, C. Jiang and T. Cai, Mechanism insight of degradation of norfloxacin by magnetite nanoparticles activated persulfate: Identification of radicals and degradation pathway, *Chem. Eng. J.*, 2017, **308**, 330-339.
8. Y. Wang, D. Tian, W. Chu, M. Li and X. Lu, Nanoscaled magnetic $CuFe_2O_4$ as an activator of peroxymonosulfate for the degradation of antibiotics norfloxacin, *Sep. Purif. Technol.*, 2019, **212**, 536-544.
9. F. Zhu, Y. Wu, Y. Liang, H. Li and W. Liang, Degradation mechanism of norfloxacin in water using persulfate activated by BC@nZVI/Ni, *Chem. Eng. J.*, 2020, **389**, 124276.
10. B. Wang, Y. N. Li and L. Wang, Metal-free activation of persulfates by corn stalk biochar for the degradation of antibiotic norfloxacin: Activation factors and degradation mechanism, *Chemosphere*, 2019, **237**, 124454.
11. Y. Zhang, H. Li, H. Huang, Q. Zhang and Q. Guo, Graphene oxide–supported cobalt phthalocyanine as heterogeneous catalyst to activate peroxymonosulfate for efficient degradation of norfloxacin antibiotics, *J. Environ. Eng.*, 2018, **144**, 04018052.
12. X. J. Wen, C. G. Niu, D.-W. Huang, L. Zhang, C. Liang and G.-M. Zeng, Study of the photocatalytic degradation pathway of norfloxacin and mineralization activity using a novel ternary Ag/AgCl-CeO_2 photocatalyst, *J. Catal.*, 2017, **355**, 73-86.
13. C. Liu, V. Nanaboina, G. V. Korshin and W. Jiang, Spectroscopic study of degradation products of ciprofloxacin, norfloxacin and lomefloxacin formed in ozonated wastewater, *Water Res.*, 2012, **46**, 5235-5246.
14. A. Tegze, G. Sági, K. Kovács, T. Tóth, E. Takács and L. Wojnárovits, Radiation induced degradation of ciprofloxacin and norfloxacin: Kinetics and product analysis, *Radiat. Phys. Chem.*, 2019, **158**, 68-75.